Sterically Protected Titanium (Aminoethyl)dicarbollides: Synthesis of Novel Constrained-Geometry Complexes Showing an Unusual Cage B,N-Cyclization

Young-Joo Lee,† Jong-Dae Lee,† Hee-Jun Jeong,† Ki-Chul Son,† Jaejung Ko,*,† Minserk Cheong,‡ and Sang Ook Kang*,†

Department of Chemistry, Korea University, 208 Seochang, Chochiwon, Chung-nam 339-700, Korea, Department of Chemistry and Research Institute for Basic Sciences, Kyung Hee University, Seoul 130-701, Korea

Received December 23, 2004

The syntheses of group 4 metal complexes containing the ((dibenzylamino)ethyl)dicarbollide ligand DcabH$^{C(2)N}$ (*nido*-7-HNBz$_2$(CH$_2$)$_2$-8-R-7,8-C$_2$B$_9$H$_{10}$; **2**) are reported. Various new types of constrained-geometry complexes [{(η^5-RC$_2$B$_9$H$_9$)(CH$_2$)$_2$(η^1-NBz$_2$)}MCl$_2$] (M = Ti (**3**), Zr (**4**); R = H (**a**), Me (**b**)) were prepared by the reaction of the potassium salt of **2** with titanium or zirconium tetrachloride. The reaction of **2** with Ti(NMe$_2$)$_4$ in toluene affords [{(η^5-RC$_2$B$_9$H$_9$)-(CH$_2$)$_2$(η^1-NBz$_2$)}Ti(NMe$_2$)$_2$] (**5**), which readily reacts with Me$_3$SiCl to yield the corresponding chloride complex **3**. The structure of the constrained-geometry complex [{(η^5-C$_2$B$_9$H$_{10}$)(CH$_2$)$_2$-(η^1-NBz$_2$)}Ti(NMe$_2$)$_2$] (**5a**) was established by X-ray diffraction, which showed an η^5:η^1 bonding mode derived from the dicarbollylamino ligand fuctional group. In contrast, the reaction of **2** with Zr(NMe$_2$)$_4$ produced the untethered half-metallocene complexes [{(η^5-RC$_2$B$_9$H$_9$)(CH$_2$)$_2$-(NBz$_2$)}Zr(NMe$_2$)$_2$(NHMe$_2$)] (**6**). The identity of **6** was confirmed by single-crystal X-ray diffraction. Due to coordination of free dimethylamine to the zirconium metal center, the sterically hindered dibenzylamine sidearm leaves the coordination sphere to form the corresponding untethered complexes. Furthermore, the titanium(IV) CGC complexes **3** exhibited unusual B,N-cyclization when reacted with O$_2$, leading to the production of novel exocyclic dicarbollides (**7**). The crystallographic data were consistent with the formation of an unusual five-membered exocyclic ring, presumably due to steric interactions between the dibenzyl units and the dicarbollyl group. Finally, the sterically less bulky zirconium(IV) ((benzylamino)ethyl)dicarbollyl complex [{(η^5-CH$_3$C$_2$B$_9$H$_9$)(CH$_2$)(η^1-NBz)}ZrCl$_2$(THF)] (**10b**), in which the pendant amine is coordinated to the metal center, was prepared by the reaction of ZrCl$_4$ with the potassium salt of [*nido*-7-NH$_2$Bz$^+$(CH$_2$)-8-H-7,8-C$_2$B$_9$H$_{10}^-$] (**9b**) in toluene.

Introduction

Dicarbollide ion is a versatile ligand and an isolobal inorganic analogue of the $C_5H_5^-$ ion. To prepare constrained-geometry catalysts with this dicarbollyl functionality is a challenging project, since incorporation of a dicarbollide fragment into the ligand framework would provide new metal/charge combinations. Therefore, recently developed constrained-geometry complexes containing both π-dicarbollyl and σ-amino or -amido components have attracted considerable attention.[1] As part of our ongoing research into the utility of the aminoalkyldicarbollyl ligand in group 4 metal chemistry, we became interested in preparing CGC-type complexes as catalyst precursors for olefin polymerization.[2] However, the strong π-donor capability of the dicarbollyl group[3]

* To whom correspondence should be addressed. Fax: 82 41 867 5396. Tel: 82 41 860 1334. E-mail: sangok@korea.ac.kr (S.O.K.).
† Korea University.
‡ Kyung Hee University.

(1) (a) Lee, Y.-J.; Lee, J.-D.; Ko, J.; Kim, S.-H.; Kang, S. O. *Chem. Commun*. **2003**, 1364. (b) Wang, J.; Vyakaranam, K.; Maguire, J. A.; Quintana, W.; Teixidor, F.; Viòas, C.; Hosmane, N. S. *J. Organomet. Chem*. **2003**, *680*, 173. (c) Kim, D.-H.; Won, J. H.; Kim, S.-J.; Ko, J.; Kim, S.-H.; Cho, S.; Kang, S. O. *Organometallics* **2001**, *20*, 4298. (d) Zhu, Y.; Vyakaranam, K.; Maguire, J. A.; Quintana, W.; Texidor, F.; Viòas, C.; Hosmane, N. S. *Inorg. Chem. Commun*. **2001**, *4*, 486.

(2) (a) McKnight, A. L.; Waymouth, R. M. *Chem. Rev*. **1998**, *98*, 2587. (b) Chen, Y.-X.; Metz, M. V.; Li, L.; Stern, C. L.; Marks, T. J. *J. Am. Chem. Soc*. **1998**, *120*, 6287. (c) Koo, K.; Marks, T. J. *J. Am. Chem. Soc*. **1998**, *120*, 4019. (d) Wang, W.; Yan, D.; Charpentier, P. A.; Zhu, S.; Hamielec, A. E.; Sayer, B. G. *Macromol. Chem. Phys*. **1998**, *199*, 2409. (e) Amor, F.; Butt, A.; du Plooy, K. E.; Spaniol, T. P.; Okuda, J. *Organometallics* **1998**, *17*, 5836. (f) Eberle, T.; Spaniol, T. P.; Okuda, J. *Eur. J. Inorg. Chem*. **1998**, 237. (g) Amor, F.; du Plooy, K. E.; Spaniol, T. P.; Okuda, J. *J. Organomet. Chem*. **1998**, *558*, 139. (h) Okuda, J.; Eberle, T. In *Metallocenes*; Halterman, R. L., Tongi, A., Eds., Wiley-VCH: Weinheim, Germany, 1998; p 415. (i) Chen, Y.-X.; Fu, P.-F.; Stern, C. L.; Marks, T. J. *Organometallics* **1997**, *16*, 5958. (j) Mu, Y.; Piers, W. E.; MacQuarrie, D. C.; Zaworotko, M. J.; Young, V. G. *Organometallics* **1996**, *15*, 2720. (k) du Plooy, K. E.; Moll, U.; Wocadlo, S.; Massa, W.; Okuda, J. *Organometallics* **1995**, *14*, 3129. (l) Okuda, J.; Schattenmann, F. J.; Wocadlo, S.; Massa, W. *Organometallics* **1995**, *14*, 789. (m) Shapiro, P. J.; Cotter, W. D.; Schaefer, W. P.; Labinger, J. A.; Bercaw, J. E. *J. Am. Chem. Soc*. **1994**, *116*, 4623. (n) Canich, J. A. M. U.S. Patent 5,026,798, 1991 (Exxon). (o) Stevens, J. C.; Timmers, F. J.; Wilson, D. R.; Schmidt, G. F.; Nickias, P. N.; Rosen, R. K.; Knight, G. A.; Lai, S. Y. Eur. Pat. Appl. 0416815 A2, 1991 (Dow). (p) Fandos, R.; Meetsma, A.; Teuben, J. H. *Organometallics* **1991**, *10*, 59. (q) Okuda, J. *Chem. Ber*. **1990**, *123*, 1649. (r) Shapiro, P. J.; Bunel, E.; Schaefer, W. P.; Bercaw, J. E. *Organometallics* **1990**, *9*, 867.

10.1021/om048979a CCC: $30.25
Publication on Web 05/10/2005

Chart 1. Previous Examples of Mono- and Bis(aminodicarbollyl) Group 4 Metal Complexes A and B

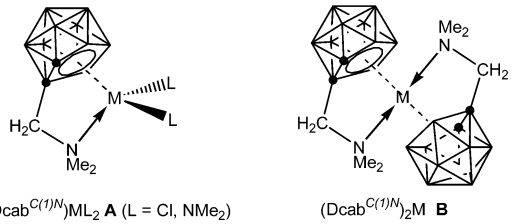

(Dcab$^{C(1)N}$)ML$_2$ **A** (L = Cl, NMe$_2$) (Dcab$^{C(1)N}$)$_2$M **B**

coupled with the inherent electrophilicity of group 4 metal centers results in the formation of the bis(dicarbollyl) complex **B** rather than the desired mono(dicarbollyl) complex **A** (Chart 1).[1b]

In an effort to block the formation of the bis(dicarbollyl) complex **B**, we attached two benzyl groups as bulky substituents onto the amino nitrogen atom. This approach was taken on the basis of the previous successful synthesis of half-sandwich group 4 metallacarboranes of diethylated C_2B_4 systems.[4] In addition, we introduced two-carbon linkers between the terminal amino nitrogen and the central dicarbollide unit, which provide an overall more flexible environment than is found in the one-carbon-chain homologues. The flexibility of this two-carbon amine arm enables strong intramolecular interaction with the metal center. In this report we describe the potential usefulness of the bulky but flexible (aminoethyl)dicarbollyl ligand in the coordination and organometallic chemistry of group 4 metals. Specifically, we describe the synthesis and structural characterization of ((dibenzylamino)ethyl)dicarbollyl group 4 CGC-type metal complexes [{(η^5-RC$_2$B$_9$H$_9$)-(CH$_2$)$_2$(η^1-NBz$_2$)}MCl$_2$] (M = Ti (**3**), Zr (**4**); R = H (**a**), Me (**b**)); to our knowledge, these complexes are the first reported examples of [Dcab$^{C(2)N}$]$^{2-}$ group 4 metal complexes with a (dibenzylamino)ethyl donor ligand (Chart 2).

Results and Discussion

We recently prepared half-sandwich metal complexes of the type [{(η^5-RC$_2$B$_9$H$_{10}$)(CH$_2$)(η^1-NMe$_2$)}TiCl$_2$] (R = H, Me; **A**),[1b] which involve η^5-dicarbollide and η^1-amine moieties. We observed that in these ligand systems, as the incoming metal becomes larger, the probability for the formation of the desired mono(dicarbollide) complex (Dcab$^{C(1)N}$)MCl$_2$ (**A**) decreases, unless specific steric factors intervene. Although coordination of [Dcab$^{C(1)N}$]$^{2-}$ reduces the electron count by 2 in theory, the thermodynamic driving force behind the formation of the bis(dicarbollide) complexes (Dcab$^{C(1)N}$)$_2$M (**B**) is the reduction of the metal's electron deficiency through the formation of the most stable bonding interactions. Thus, in the present work we have incoporated bulky substituents on the dicarbollyl ligand in order to block the formation of 16-electron bis(dicarbollide) complexes **B**.

Chart 2. Modified ((Dibenzylamino)ethyl)-dicarbollyl Group 4 Metal Complexes 3 and 4

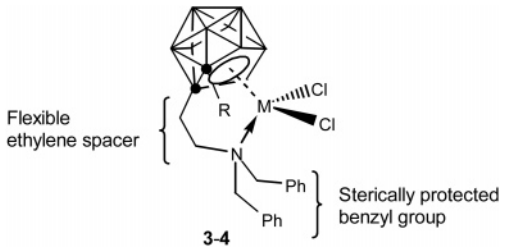

3-4

Scheme 1. Generation of the Sterically Protected (Aminoethyl)dicarbollyl Ligand 2[a]

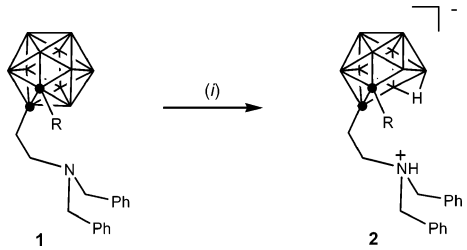

[a] Conditions: (i) (a) KOH, EtOH, 78 °C; (b) H_3PO_4, benzene, 25 °C, 10 h (R = H (**a**), CH_3 (**b**)).

Ligand Synthesis. New ((dibenzylamino)ethyl)dicarbollyl ligands, abbreviated as DcabH$^{C(2)N}$ (**2**), were prepared by applying a standard deboronation procedure[5] to (aminoethyl)-*o*-carborane (*closo*-1-NBz$_2$(CH$_2$)$_2$-2-R-1,2-C$_2$B$_{10}$H$_{10}$) (R = H (**1a**), Me (**1b**)) (Scheme 1).[6] In this procedure, reaction of **1** with KOH in ethanol at 78 °C and subsequent protonation with phosphoric acid leads to the formation of deboronated zwitterionic compounds (**2**). An X-ray structural determination carried out on the crystals produced by this reaction revealed the formula of the salts to be the zwitterionic form *nido*-7-NHBz$_2^+$(CH$_2$)$_2$-8-R-7,8-C$_2$B$_9$H$_{10}^-$. Figures 1 and 2 show the conformation of the (dibenzylamino)-ethyl-tethered open dicarbollide structures of **2a** and **2b**, respectively; the availability of potential multidentate η^5:η^1-dicarbollylamino ligand functionalities can clearly be discerned in these structures.

Spectroscopic characterization of these complexes shows that the aminoethyl group is linked to the nido cage carborane. The characteristic asymmetric pattern in the ^{11}B{^{1}H} NMR spectrum in the range −12 to −39 ppm and the presence of an absorption at ∼−3.0 ppm in the ^{1}H NMR spectrum imply a B−H−B interaction on the C$_2$B$_3$ open face. Most importantly, the ^{1}H NMR spectra of these complexes display a singlet pattern for the α-positioned methylene units to the amino nitrogen atom, at around 4.3 ppm for the two NC*H*$_2$Ph groups and at around 3.0 ppm for the NC*H*$_2$CH$_2$ group. Further deprotonation of this bridge hydrogen with KH gives the corresponding dianionic ligand Dcab$^{C(2)N}$ ([*nido*-7-NBz$_2$(CH$_2$)$_2$-8-R-7,8-C$_2$B$_9$H$_9$]$^{2-}$).

(3) (a) Bei, X.; Kreuder, C.; Swenson, D. C.; Jordan, R. F.; Young, V. G., Jr. *Organometallics* **1998**, *17*, 1085. (b) Yoshida, M.; Jordan, R. F. *Organometallics* **1997**, *16*, 4508. (c) Yoshida, M.; Crowther, D. J.; Jordan, R. F. *Organometallics* **1997**, *16*, 1349. (d) Crowther, D. J.; Swenson, D. C.; Jordan, R. F. *J. Am. Chem. Soc*. **1995**, *117*, 10403. (e) Bowen, D. E.; Jordan, R. F.; Rogers, R. D. *Organometallics* **1995**, *14*, 3630. (f) Kreuder, C.; Jordan, R. F.; Zhang, H. *Organometallics* **1995**, *14*, 2993. (g) Uhrhammer, R.; Su, Y.-X.; Swenson, D. C.; Jordan, R. F. *Inorg. Chem*. **1994**, *33*, 4398. (h) Bazan, G. C.; Schaefer, W. P.; Bercaw, J. E. *Organometallics* **1993**, *12*, 2126. (i) Uhrhammer, R.; Crowther, D. J.; Olson, J. D.; Swenson, D. C.; Jordan, R. F. *Organometallics* **1992**, *11*, 3098. (j) Crowther, D. J.; Baenziger, N. C.; Jordan, R. F. *J. Am. Chem. Soc*. **1991**, *113*, 1455.

(4) Dodge, T.; Curtis, M. A.; Russell, J. M.; Sabat, M.; Finn, M. G.; Grimes, R. N. *J. Am. Chem. Soc*. **2000**, *122*, 10573.

(5) (a) Plesek, J.; Hermanek, S.; Stibr, B. *Inorg. Synth*. **1983**, *22*, 231. (b) Wiesboeck, R. A.; Hawthorne, M. F. *J. Am. Chem. Soc*. **1964**, *86*, 1642.

(6) Lee, J.-D.; Lee, Y.-J.; Jeong, H.-J.; Lee, J. S.; Lee, C.-H.; Ko, J.; Kang, S. O. *Organometallics* **2003**, *22*, 445.

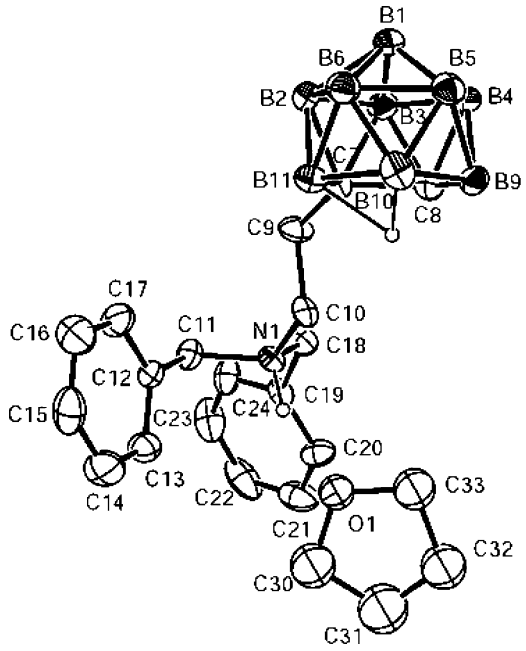

Figure 1. Molecular structure of **2a**·C_4H_8O with thermal ellipsoids drawn at the 30% level.

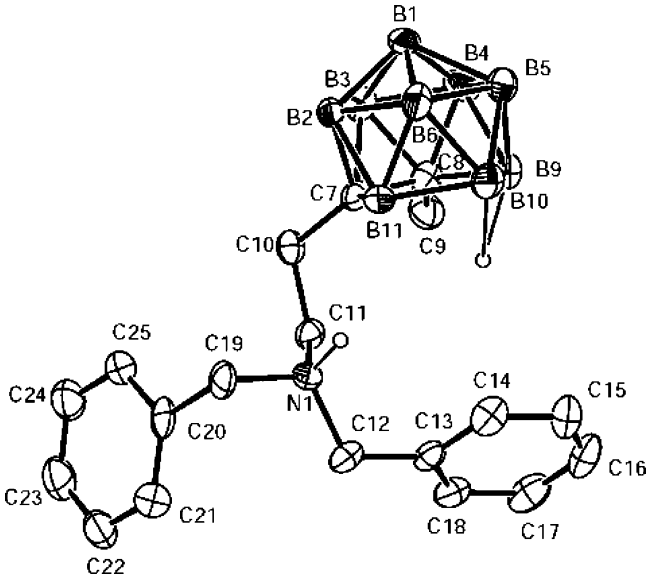

Figure 2. Molecular structure of **2b** with thermal ellipsoids drawn at the 30% level.

Reaction of the Ligand with Group 4 Metal Complexes MX_4. Reaction of the potassium salt of **2** with MCl_4 (M = Ti, Zr) in toluene gives new compounds, formulated as the mono(dicarbollyl) species [{(η^5-$RC_2B_9H_9$)$(CH_2)_2$(η^1-NBz_2)}MCl_2] (**3** and **4**; Scheme 2).

The precise structures of these compounds are unknown, due to our inability to obtain single crystals for X-ray analysis; complexes **3** and **4** slowly decomposed in solution or during crystallization. However, mass spectrometry confirmed the above formulation. Several structural features were established from the spectral data of **3** and **4**. The deprotonation of the ligand **2** was evident from the disappearance of the bridge hydrogens of B−H−B and N−H (^{1}H NMR: δ −3.0 and 9.46). The methylene protons of the NCH_2 groups in **3** and **4** are diastereotopic, each giving rise to an AB spin pattern. The most significant difference between the ^{1}H NMR spectra of **2** and those of **3** and **4** is observed in the low-field shift of the signals due to the respective methylene hydrogens of the NCH_2CH_2 unit: for complex **2**, these signals are observed at around δ 3.0, whereas for **3** and **4** they occur at δ 4.0−4.2. The signals for the methylene protons of the benzyl groups attached to the nitrogen atom are also shifted downfield (δ 4.5−4.7). Corresponding downfield shifts for the methylene groups adjacent to the nitrogen atom are also observed in the ^{13}C NMR spectra. This observation is consistent with similar findings for other intramolecularly coordinated metal complexes that contain methylene spacers such as ($Dcab^{C(1)N}$)ML_2 (M = Ti, L = Cl;[1b] M = Fe, Ru, L = Lewis base;[7] M = Ni, L = PPh_3[8]). In addition, the ^{11}B chemical shifts are similar to those observed for other dicarbollylmetal complexes and support the proposed η^5 coordination.[3,9] The spectroscopic data for complexes **3** and **4** indicate that the dibenzylamino group of the side

Scheme 2. Synthesis of Group 4 Metal CGC-Type Complexes Derived from the (Aminoethyl)dicarbollyl Ligand 2[a]

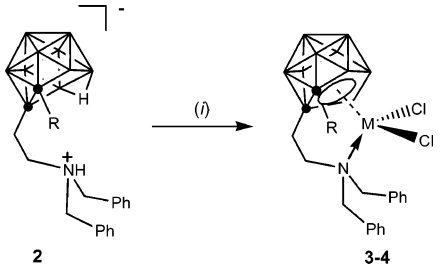

[a] Conditions: (i) (a) KH, THF, 0 °C; (b) MCl_4, toluene, −78 °C (M = Ti (**3**), Zr (**4**); R = H (**a**), CH_3 (**b**)).

Scheme 3. Alternate Synthetic Route for the Formation of Group 4 Metal CGC Complexes[a]

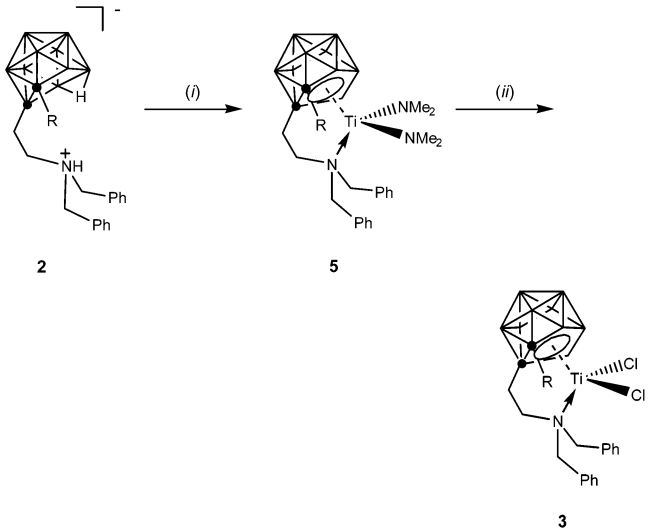

[a] Conditions: (i) $Ti(NMe_2)_4$, toluene, 25 °C; (ii) Me_3SiCl, CH_2Cl_2, 25 °C (R = H (**a**), Me (**b**)).

(7) Park, J.-S.; Kim, D.-H.; Ko, J.; Kim, S. H.; Cho, S.; Lee, C.-H.; Kang, S. O. *Organometallics* **2001**, *20*, 4642.

(8) Park, J.-S.; Kim, D.-H.; Kim, S.-J.; Ko, J.; Kim, S. H.; Cho, S.; Lee, C.-H.; Kang, S. O. *Organometallics* **2001**, *20*, 4483.

(9) (a) Su, Y.-X.; Reck, C. E.; Guzei, I. A.; Jordan, R. F. *Organometallics* **2000**, *19*, 4858. (b) Houseknecht, K. L.; Stockman, K. E.; Sabat, M.; Finn, M. G.; Grimes, R. N. *J. Am. Chem. Soc.* **1995**, *117*, 1163. (c) Oki, A. R.; Zhang, H.; Hosmane, N. S. *Organometallics* **1991**, *10*, 3964. (d) Manning, M. J.; Knobler, C. B.; Khatter, R.; Hawthorne, M. F. *Inorg. Chem.* **1991**, *30*, 2009. (e) Siriwardane, U.; Zhang, H.; Hosmane, N. S. *J. Am. Chem. Soc.* **1990**, *112*, 9637.

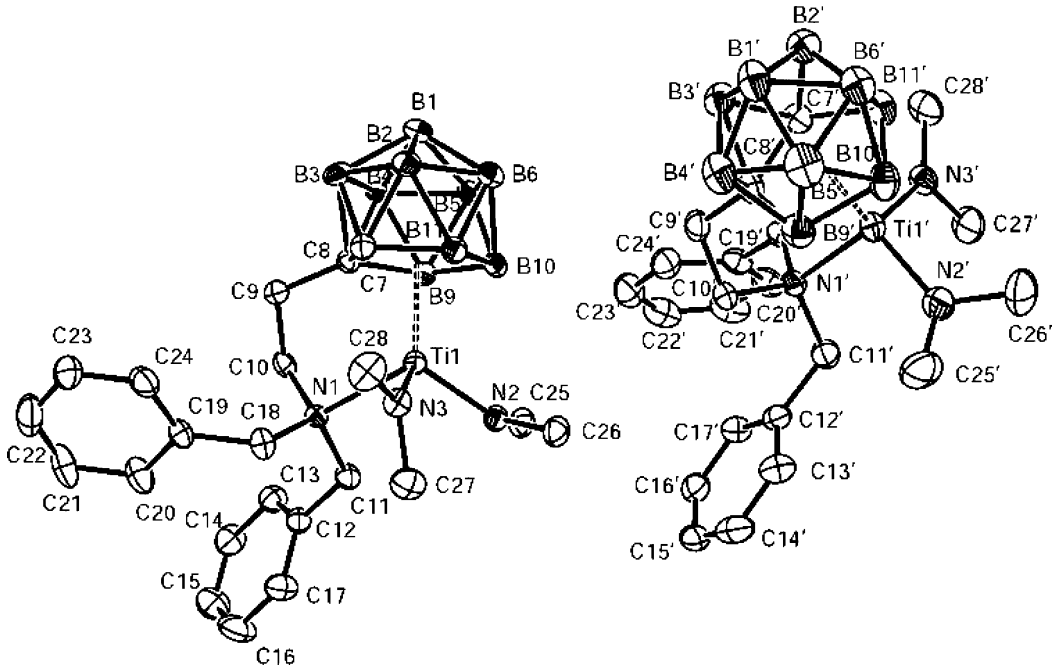

Figure 3. Molecular structure of **5a** with thermal ellipsoids drawn at the 30% level.

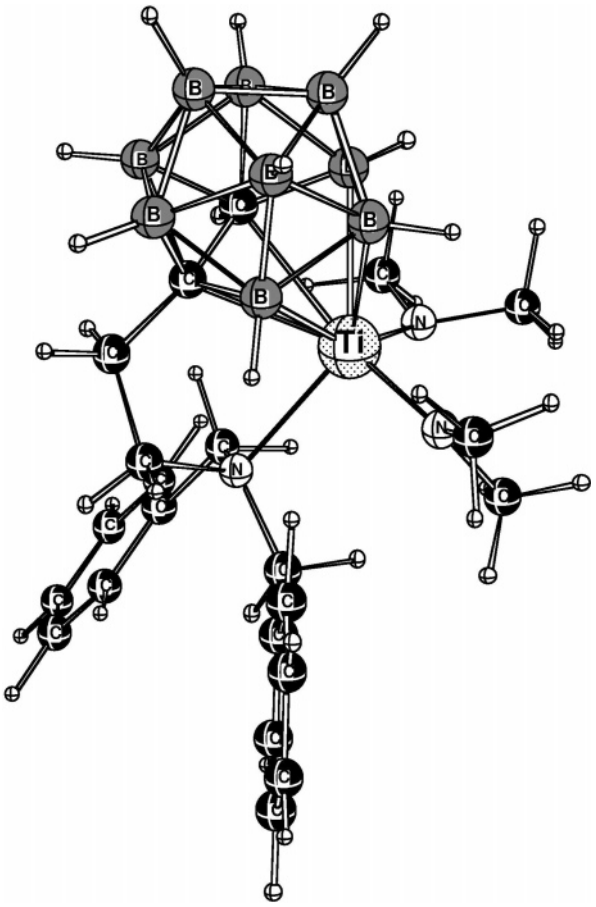

Figure 4. DFT-optimized structure of **5a** with atom-labeling scheme.

chain is coordinated to the metal center in all cases. Compounds **3** and **4** represent the first examples of dicarbollyl group 4 metal complexes with intramolecular coordination of a (dibenzylamino)ethyl donor function in the side chain. Thus, all four of the new dicarbollyl-amino complexes **3** and **4** were prepared from the

Scheme 4. Isolation of Untethered Piano-Stool Zirconium Complexes[a]

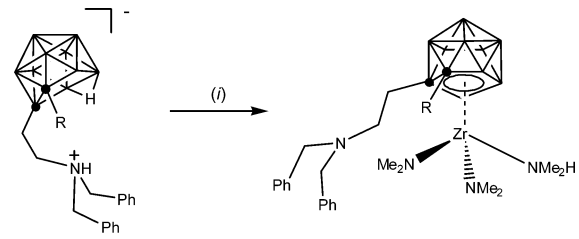

2 **6**

[a] Conditions: (i) $Zr(NMe_2)_4$, toluene, 25 °C (R = H (**a**), Me (**b**)).

requisite group 4 complex MX_4 (M = Ti, Zr) and an equivalent amount of nucleophile **2** in toluene solutions, as shown in Scheme 2. The pure products, which ranged from red to dark red in color, were isolated by recrystallization. Typically, the yields of **3** and **4** were on the order of 23−29%.

We have examined the use of these complexes for the polymerization of ethylene. Unfortunately, all four complexes (**3** and **4**) exhibited poor catalytic activities for the polymerization process, ranging from 340 to 1150 kg of PE $mol_{cat}^{-1}\ h^{-1}$ for reaction conditions at variable temperatures (25, 60, 100 °C) and 100 psig of ethylene. Independent experiments showed these complexes were easily decomposed under the conditions of catalysis, accounting for the low catalytic activity (see the Supporting Information).

Due to the low-yield conversion to titanium complexes, we devised a direct metalation process with the zwitterionic (aminoethyl)dicarbollide $DcabH^{C(2)N}$ (**2**). As shown in Scheme 3, reaction of **2** with $Ti(NMe_2)_4$ in toluene produced the desired mono(dicarbollide) complex $(Dcab^{C(2)N})Ti(NMe_2)_2$ (**5**) in good yields (73−81%). The corresponding chlorinated derivatives $(Dcab^{C(2)N})$-$TiCl_2$ (**3**) were prepared from the amido complexes **5** and a slight excess of Me_3SiCl in CH_2Cl_2 solution. This new procedure gave the desired CGC complexes **3** in much

Table 1. NMR Spectroscopic Data for Compounds 2−7, 9b. and 10b

compd	NMR (δ)		
	^{1}H	^{13}C	^{11}B
2a[a]	9.46 (br, 1H, N−*H*)	131.12, 129.88, 128.99 (NCH$_2$*Ph*)	−12.85 (3B)
	7.48, 7.37, 7.36 (10H, NCH$_2$*Ph*)	56.14 (N*C*H$_2$Ph)	−18.06 (2B)
	4.30 (s, 4H, NC*H*$_2$Ph)	45.01 (CH$_2$*C*H$_2$N)	−21.21 (2B)
	2.96 (br, 2H, CH$_2$C*H*$_2$N)	31.53 (*C*H$_2$CH$_2$N)	−35.19 (1B)
	1.90 (br, 2H, C*H*$_2$CH$_2$N)		−39.02 (1B)
	1.51 (s, 1H, C$_{cab}$−*H*)		
	−3.12 (br, 1H, 1H, B−*H*−B)		
2b[a]	9.46 (br, 1H, N−*H*)	131.32, 129.91, 129.66, 129.14 (NCH$_2$*Ph*)	−11.92 (3B)
	7.49, 7.48, 7.36 (10H, NCH$_2$*Ph*)	56.54 (N*C*H$_2$Ph)	−19.96 (3B)
	4.35 (s, 4H, NC*H*$_2$Ph)	50.64 (CH$_2$*C*H$_2$N)	−36.66 (1B)
	3.01 (br, 2H, CH$_2$C*H*$_2$N)	28.36 (*C*H$_2$CH$_2$N)	−38.18 (1B)
	1.96 (br, 2H, C*H*$_2$CH$_2$N)	21.42 (C$_{cab}$−*Me*)	−39.19 (1B)
	1.11 (s, 3H, C$_{cab}$−*Me*)		
	−2.91 (br, 1H, B−*H*−B)		
3a[c]	7.56, 7.52, 7.51, 7.50, 7.48, 7.46 (10H, NCH$_2$*Ph*)	133.04, 132.45, 130.15, 129.92, 127.74, 127.65 (NCH$_2$*Ph*)	1.95 (1B)
	4.66 (d, 2H, NC*H*$_2$Ph, $^{2}J_{H-H}$ = 14 Hz)	68.42 (N*C*H$_2$Ph)	−16.35 (3B)
	4.49 (d, 2H, NC*H*$_2$Ph, $^{2}J_{H-H}$ = 14 Hz)	64.27 (N*C*H$_2$Ph)	−26.65 (1B)
	4.17 (m, 1H, CH$_2$C*H*$_2$N)	50.41 (CH$_2$*C*H$_2$N)	−31.18 (1B)
	4.06 (m, 1H, CH$_2$C*H*$_2$N)	40.84 (*C*H$_2$CH$_2$N)	−38.50 (1B)
	2.14 (br, 1H, C*H*$_2$CH$_2$N)		−44.63 (2B)
	1.94 (br, 1H, C*H*$_2$CH$_2$N)		
	1.47 (br, 1H, C$_{cab}$-*H*)		
3b[c]	7.53, 7.49, 7.47, 7.44, 7.39 (10H, NCH$_2$*Ph*)	135.27, 134.11, 132.87, 130.71, 130.23, 129.87, 127.91, 126.51 (NCH$_2$*Ph*)	1.93 (1B)
	4.53 (d, 2H, NC*H*$_2$Ph, $^{2}J_{H-H}$ = 15 Hz)	72.82 (N*C*H$_2$Ph)	−15.34 (2B)
	4.49 (d, 2H, NC*H*$_2$Ph, $^{2}J_{H-H}$ = 15 Hz)	70.44 (N*C*H$_2$Ph)	−24.10 (2B)
	4.19 (m, 1H, CH$_2$C*H*$_2$N)	54.14 (CH$_2$*C*H$_2$N)	−35.27 (2B)
	4.01 (m, 1H, CH$_2$C*H*$_2$N)	40.03 (*C*H$_2$CH$_2$N)	−40.84 (1B)
	2.19 (br, 1H, C*H*$_2$CH$_2$N)	24.59 (C$_{cab}$−*Me*)	−43.24 (1B)
	1.96 (br, 1H, C*H*$_2$CH$_2$N)		
	1.30 (br, 3H, C$_{cab}$−*Me*)		
4a[c]	7.57, 7.50 (10H, NCH$_2$*Ph*)	139.94, 138.02, 132.91, 132.37, 131.44, 129.10, 127.97 (NCH$_2$*Ph*)	4.88 (1B)
	4.65 (d, 2H, NC*H*$_2$Ph, $^{2}J_{H-H}$ = 15 Hz)	59.66 (N*C*H$_2$Ph)	−1.38 (1B)
	4.45 (d, 2H, NC*H*$_2$Ph, $^{2}J_{H-H}$ =15 Hz)	53.86 (CH$_2$*C*H$_2$N)	−12.36 (3B)
	4.18 (m, 1H, CH$_2$C*H*$_2$N)	35.53 (*C*H$_2$CH$_2$N)	−19.34 (3B)
	4.05 (m, 1H, CH$_2$C*H*$_2$N)		−44.03 (1B)
	2.12 (br, 1H, C*H*$_2$CH$_2$N)		
	2.02 (br, 1H, C*H*$_2$CH$_2$N)		
	1.48 (br, 1H, C$_{cab}$−*H*)		
4b[c]	7.57, 7.50 (10H, NCH$_2$*Ph*)	138.00, 132.48, 131.99, 131.08, 130.69, 130.22, 129.37, 127.81, 127.69 (NCH$_2$*Ph*)	1.68 (1B)
	4.72 (d, 2H, NC*H*$_2$Ph, $^{2}J_{H-H}$ = 12 Hz)	60.68 (N*C*H$_2$Ph)	−6.73 (1B)
	4.50 (d, 2H, NC*H*$_2$Ph, $^{2}J_{H-H}$ = 12 Hz)	54.32 (CH$_2$*C*H$_2$N)	−11.54 (3B)
	4.20 (m, 1H, CH$_2$C*H*$_2$N)	34.10 (*C*H$_2$CH$_2$N)	−17.53 (3B)
	3.95 (m, 1H, CH$_2$C*H*$_2$N)	29.64 (C$_{cab}$−*Me*)	−43.42 (1B)
	3.42 (br, 1H, C*H*$_2$CH$_2$N)		
	3.13 (br, 1H, C*H*$_2$CH$_2$N)		
	1.18 (br, 1H, C$_{cab}$−*Me*)		
5a[c]	7.38, 7.21, 7.19, 7.14, 7.07, 7.03 (m, 10H, NCH$_2$*Ph*)	139.06, 129.74, 129.06, 126.84, 124.98 (NCH$_2$*Ph*)	−17.79 (3B)
		61.87 (N*C*H$_2$Ph)	−24.04 (2B)
	3.56 (s, 12H, Ti(N*Me*$_2$)$_2$)	58.48 (Ti(N*Me*$_2$)$_2$)	−26.69 (2B)
	3.44 (s, 4H, NC*H*$_2$Ph)	56.71 (CH$_2$*C*H$_2$N)	−40.02 (1B)
	2.88 (m, 2H, CH$_2$C*H*$_2$N)	35.89 (*C*H$_2$CH$_2$N)	−43.55 (1B)
	2.22 (m, 2H, C*H*$_2$CH$_2$N)		
	1.37 (s, 1H, C$_{cab}$−*H*)		
5b[b]	7.42, 7.40, 7.37, 7.34, 7.32, 7.30 (10H, NCH$_2$*Ph*)	140.18, 139.28, 132.52, 132.23, 131.19, 125.99 (NCH$_2$*Ph*)	3.06 (1B)
	3.52 (s, 12H, Ti(N*Me*$_2$)$_2$)	61.50 (N*C*H$_2$Ph)	−16.97 (3B)
	3.31 (s, 2H, NC*H*$_2$Ph)	58.28 (Ti(N*Me*$_2$)$_2$)	−25.22 (2B)
	2.59 (m, 2H, CH$_2$C*H*$_2$N)	48.22 (CH$_2$*C*H$_2$N)	−37.38 (1B)
	2.18 (m, 2H, C*H*$_2$CH$_2$N)	32.58 (*C*H$_2$CH$_2$N)	−41.36 (1B)
	1.58 (s, 3H, C$_{cab}$−*Me*)	22.80 (C$_{cab}$−*Me*)	−44.41 (1B)
6a[b]	7.30, 7.27, 7.19 (10H, NCH$_2$*Ph*)	138.50, 129.64, 128.89, 128.09, 126.94 (NCH$_2$*Ph*)	−6.21 (1B)
	3.60 (s, 2H, NC*H*$_2$Ph)	66.85 (N*C*H$_2$Ph)	−9.29 (1B)
	3.07 (s, 12H, Zr(N*Me*$_2$)$_2$)	59.00 (Zr(N*Me*$_2$)$_2$)	−14.48 (4B)
	2.70(s, 6H, ZrNH*Me*$_2$)	54.06 (Zr(N*Me*$_2$H))	−18.13 (2B)
	2.61(br, 1H, ZrN*H*Me$_2$)	41.96 (CH$_2$*C*H$_2$N)	−28.39 (1B)
	2.51(br, 2H, CH$_2$C*H*$_2$N)	33.89 (*C*H$_2$CH$_2$N)	
	1.78(br, 2H, C*H*$_2$CH$_2$N)		
	1.15(s, 1H, C$_{cab}$−*H*)		

Table 1 (Continued)

compd	NMR (δ) ^{1}H	^{13}C	^{11}B
6b[b]	7.34, 7.28, 7.21, 7.15, 7.11 (m, 10H, NCH_2Ph)	131.51, 130.35, 129.64, 127.90, 127.19 (NCH_2Ph)	−7.80 (1B)
	3.70 (s, 2H, NCH_2Ph)	69.04 (NCH_2Ph)	−10.80 (3B)
	3.26 (s, 12H, $Zr(NMe_2)_2$)	58.27 ($Zr(NMe_2)_2$)	−12.08 (3B)
	2.87 (br, 2H, CH_2CH_2N)	55.18 ($ZrNHMe_2$)	−16.92 (1B)
	2.62 (s, 6H, $ZrNHMe_2$)	45.13 (CH_2CH_2N)	−28.92 (1B)
	2.34 (br, 1H, $ZrNHMe_2$)	33.30 (CH_2CH_2N)	
	2.26 (br, 2H, CH_2CH_2N)	24.51 ($C_{cab}-Me$)	
	1.97 (s, 3H, $C_{cab}-Me$)		
7a[b]	7.52, 7.50, 7.48, 7.47, 7.45 (10H, NCH_2Ph)	132.92, 132.27, 130.77, 130.15, 129.92, 129.61, 129.39, 129.02 (NCH_2Ph)	0.89 (1B)
	4.53 (d, 1H, NCH_2Ph, $^2J_{H-H}$ = 13 Hz)	66.27 (NCH_2Ph)	−8.67 (1B)
	4.39 (d, 1H, NCH_2Ph, $^2J_{H-H}$ = 13 Hz)	64.26 (NCH_2Ph)	−15.91 (1B)
	4.22 (d, 1H, NCH_2Ph, $^2J_{H-H}$ = 13 Hz)	31.79 (CH_2CH_2N)	−21.36 (1B)
	4.15 (d, 1H, NCH_2Ph, $^2J_{H-H}$ = 13 Hz)		−27.53 (2B)
	3.44 (m, 1H, CH_2CH_2N)[d]		−36.57 (1B)
	3.31 (m, 1H, CH_2CH_2N)[d]		−39.40 (1B)
	1.86 (m, 2H, CH_2CH_2N)		−42.85 (1B)
	1.67 (s, 1H, $C_{cab}-H$)		
7b[b]	7.61, 7.60, 7.58, 7.56, 7.48, 7.47, 7.46, 7.44, 7.42 (10H, NCH_2Ph)	133.52, 132.50, 131.19, 130.25, 129.64, 129.29, 128.77, 127.65 (NCH_2Ph)	−5.29 (2B)
	4.58 (d, 1H, NCH_2Ph, $^2J_{H-H}$ = 14 Hz)	66.31 (NCH_2Ph)	−18.71 (1B)
	4.52 (d, 1H, NCH_2Ph, $^2J_{H-H}$ = 14 Hz)	63.12 (NCH_2Ph)	−24.68 (2B)
	4.50 (d, 1H, NCH_2Ph, $^2J_{HH}$ = 12 Hz)	34.34 (CH_2CH_2N)	−34.71 (2B)
	4.43 (d, 1H, NCH_2Ph, $^2J_{H-H}$ = 12 Hz)	29.53 ($C_{cab}-Me$)	−40.88 (1B)
	3.43 (m, 1H, CH_2CH_2N)[d]		−48.70 (1B)
	3.35 (m, 1H, CH_2CH_2N)[d]		
	1.63 (m, 2H, CH_2CH_2N)		
	1.14 (s, 3H, $C_{cab}-Me$)		
9b[a]	8.57 (br, 2H, $N-H$)	132.13, 130.04, 129.53, 129.02, 128.67, 128.46 (NCH_2Ph)	−15.68 (3B)
	7.47, 7.45, 7.35 (5H, NCH_2Ph)	57.73 (NCH_2Ph)	−23.91 (3B)
	4.17 (s, 2H, NCH_2Ph)	50.01 (CH_2CH_2N)	−40.60 (1B)
	2.97 (br, 2H, CH_2CH_2N)	30.70 (CH_2CH_2N)	−42.04 (1B)
	1.92 (d, 2H, CH_2CH_2N)	21.52 ($C_{cab}-Me$)	−43.41 (1B)
	1.36 (s, 3H, $C_{cab}-Me$)		
	−2.89 (br, 1H, $B-H-B$)		
10b[b]	7.50, 7.40, 7.35, 7.28, 7.23 (5H, NCH_2Ph)	129.66, 128.93, 128.53, 127.90 (NCH_2Ph)	6.99 (2B)
	4.67 (m, 2H, NCH_2Ph)	71.96 (NCH_2Ph)	−8.23 (3B)
	3.76 (m, 2H, THF)	67.97 (THF)	−17.70 (2B)
	3.58 (m, 1H, CH_2CH_2N)	51.88 (NCH_2Ph)	−24.85 (2B)
	3.54 (m, 1H, CH_2CH_2N)	39.21 (CH_2CH_2N)	
	3.38 (m, 1H, CH_2CH_2N)	26.08 ($C_{cab}-Me$)	
	3.18 (m, 1H, CH_2CH_2N)	25.62 (THF)	
	2.55 (br, 1H, $N-H$)		
	1.87 (m, 2H, THF)		
	1.26 (s, 3H, $C_{cab}-Me$)		

[a] $(CD_3)_2SO$ was used as the solvent, and the chemical shifts are reported relative to the residual H of the solvent. [b] $CDCl_3$ was used as the solvent, and the chemical shifts are reported relative to the residual H of the solvent. [c] C_6D_6 was used as the solvent, and the chemical shifts are reported relative to the residual H of the solvent. [d] Due to the extensive overlapping of the peaks, a coupling constant cannot be determined.

higher yield than was achieved using the reaction described in Scheme 2. We believe that the metathesis reaction involving the potassium salt of **2** showed a complex redox reaction with titanium tetrachloride.

An X-ray structural determination confirmed the expected constrained-geometry species illustrated in Figure 3, wherein an asymmetric unit contains two independent molecules of **5a**. Overall, **5a** adopts a characteristic three-legged "piano stool" structure with the titanium atom η^5 coordinated on one side by a nido-dicarbollyl group and on the other by the dibenzylamino group and two dimethylamido ligands. The overall geometry is similar to that found in the complex (η^5-$C_2B_9H_{11}$)$Ti(NMe_2)_2(HNMe_2)$.[10] The short Ti(1)−N(2)/Ti(1′)−N(2′) and Ti(1)−N(3)/Ti(1′)−N(3′) bond distances (1.896(3)/1.888(3) Å and 1.916(3)/1.901(3) Å) and the planar geometry around the N(2)/N(2′) and N(3)/N(3′) nitrogen atoms indicate that both nitrogen atoms with sp^2 hybridization are engaged in N(pπ)→Ti(dπ) interactions.[11] Observation of a Ti(1)−N(1)/Ti(1)−N(1′) distance of 2.319(3)/2.310(3) Å, which is consistent with a Ti−N(sp^3) single bond,[12] confirms that the N-donor atom is coordinated to the metal in a strain-free manner. The Ti−C_2B_3(cent) distance (1.936/1.943 Å) in **5a** (where C_2B_3(cent) is the centroid of the dicarbollyl ring) is similar to that found in the complex (η^5-$C_2B_9H_{11}$)(η^5-C_5Me_5)Ti(N=CMe_2) (1.91 Å) and approximately 0.1 Å shorter than the corresponding value for (η^5-$C_2B_9H_{11}$)(η^5-C_5Me_5)Ti(N=CMe_2)(MeCN) (2.02 Å), due to the lower coordination number.[3f] The two dimethylamido ligands

(10) Zi, G.; Li, H.-W.; Xie, Z. *Organometallics* **2002**, *21*, 3850.

(11) Wang, H.; Wang, Y.; Li, H.-W.; Xie, Z. *Organometallics* **2001**, *20*, 5110.

(12) Kwong, W.-C.; Chan, H.-S.; Tang, Y.; Xie, Z. *Organometallics* **2004**, *23*, 4301.

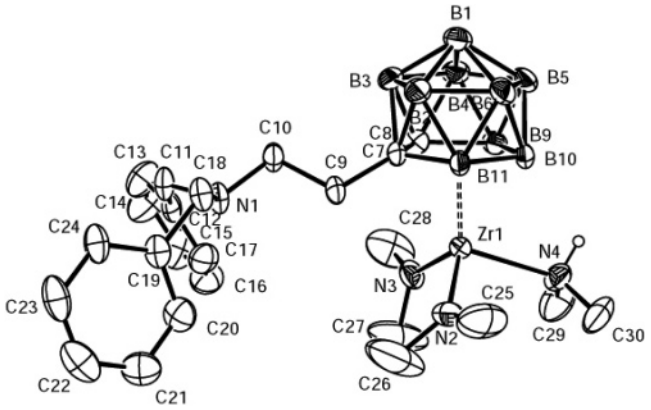

Figure 5. Molecular structure of **6a** with thermal ellipsoids drawn at the 30% level.

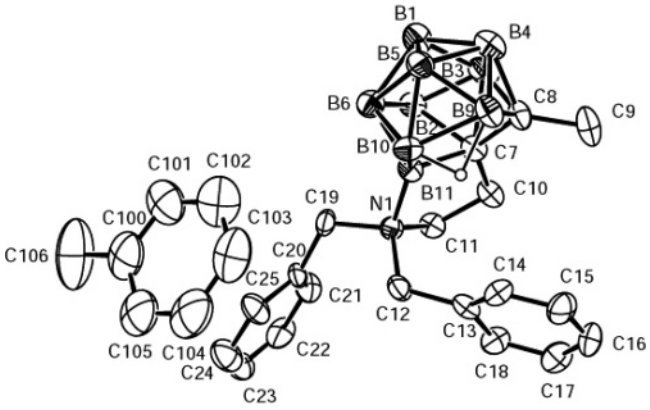

Figure 6. Molecular structure of **7b**·C_7H_8 with thermal ellipsoids drawn at the 30% level.

are oriented so that these groups face away from the (dibenzylamino)ethyl group bound at the dicarbollyl unit. Thus, the preferred formation of a mono- over a bis(dicarbollyl) complex can be ascribed to the greater steric protection afforded by the dibenzyl unit as compared to the methyl group on the sidearm nitrogen atom of **A**.

To examine the stabilizing influence of the chelating (dibenzylamino)ethyl dicarbollyl ligand on **5a**, we performed a series of density functional calculations on the model complex **5a**, the optimized structure of which is shown in Figure 4. These calculations confirmed that the structure of **5a** fits quite neatly with the pseudotetrahedral geometry of the model ML_4 complex.[13] The main structural features of the calculated geometry of **5a**, including the most significant geometrical parameters, are in good agreement with those determined by X-ray crystallographic methods (see the Supporting Information).

In contrast to the above reactions, where two amine ligands are eliminated from $Ti(NMe_2)_4$ in the presence of the multidentate ligand $DcabH_2^{C(2)N}$ (**2**), treatment of $Zr(NMe_2)_4$ with **2** gave the untethered complexes **6** in good yield (Scheme 4).

The detachment of the sidearm during the reaction in Scheme 4 was evident from change in the signal corresponding to the bridgehead methylene unit in the ^{1}H NMR spectrum from AB to a broad singlet pattern. Compounds **6a** and **6b** were readily identified from their spectroscopic properties (Table 1). The amine Me moieties of **6** were recognized from features in the ^{1}H NMR spectra at the characteristic positions of δ 2.70 (**6a**) and 2.62 (**6b**). The X-ray crystal structure of **6a**, shown in Figure 5, reveals that the Zr atom essentially adopts an η^5 bonding mode with the dicarbollyl rings and an η^1 bonding mode with the two dimethylamido ligands and dimethylamine ligand. In particular, structural studies revealed that the dimethylamine freed from $Zr(NMe_2)_4$ was recoordinated to the zirconium atom of **6** in one leg position of the piano-stool geometry. The formation of **6** presumably results from attachment of a liberated amine ligand and concomitant detachment of a dibenzylamine unit of the sidearm by a ligand substitution reaction. The noticeable shortening of the Zr−C_2B_3(cent) distance (2.109 Å) (where C_2B_3(cent) is the centroid of the dicarbollyl ring) and the expansion of the N(2)−Zr(1)−N(3) (107.1(2)°) and N(4)−Zr(1)−N(2)/N(4)−Zr−N(3) (100.4(2)/96.8(2)°) angles in **6a** can be explained by the steric relief caused by the detachment of the bulky dibenzylamino sidearm. In **6a**, the Zr(1)−N(2)/Zr(1)−N(3) distance is 2.029(4)/2.020(4) Å and Zr−N(4) = 2.363(4) Å, compared to 1.90 and 2.31 Å, respectively, in (η^5-$C_2B_9H_{11}$)$Zr(NEt_2)_2(HNEt_2)$.[3e] As expected, the Zr−N_{amino} distance (2.36 Å) is much longer than the Zr−N_{amido} distance (2.02 Å)[10,11,14] and N(4) adopts a pyramidal geometry. In addition, it was deduced that the metal-appended dibenzyl group had uncomplexed to the untethered form; indeed, this arrangement, in which the (dibenzylamino)ethyl substituents are in a remote disposition, is arguably a favorable form.

Scheme 5. Unexpected Formation of Fused Exocyclic Dicarbollyl Compounds[a]

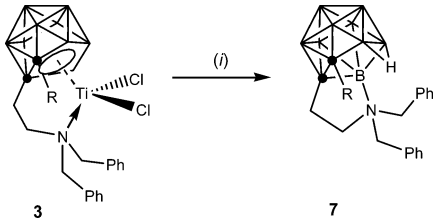

3 **7**

[a] Conditions: (i) O_2, toluene, 25 °C (R = H (**a**), Me (**b**)).

The most interesting property of **3** is its reaction with oxygen and transformation to **7**. Compound **7** was initially isolated in the synthesis of **3** as a minor yellow product. In fact, we have found that reactions of **3** with O_2 always proceed in moderate yields, as determined by ^{1}H NMR spectroscopy.

An X-ray study of **7b** (Figure 6) revealed it to be an exocyclic dicarbollide compound containing an unusual five-membered B,N-cyclized ring derived from tethering of the amino group (Scheme 5). The tertiary amino fragment coordinates to one of the borons in the remaining basal site of the open C_2B_3 face, giving a fused five-membered ring. The C_2B_3 bonding face and exocyclic five-membered C_3BN ring in **7b** are essentially planar, with deviations from the least-squares plane of less than 0.123 and 0.203 Å, respectively. The angle between the two five-membered fused rings is 154.02°.

(13) Beddie, C.; Hollink, E.; Wei, P.; Gauld, J.; Stephan, D. W. *Organometallics* **2004**, *23*, 5240.

(14) (a) Wang, Y.; Wang, H.; Li, H.-W.; Xie, Z. *Organometallics* **2002**, *21*, 3311. (b) Lee, M. H.; Hwang, J.-W.; Kim, Y.; Han, Y.; Do, Y. *Organometallics* **2000**, *19*, 5514.

Table 2. X-ray Crystallographic Data and Processing Parameters for Compounds 2a·C_4H_8O, 2b, 5a, 6a, 7b·C_7H_8, 9b, and 10b

	2a·C_4H_8O	**2b**	**5a**	**6a**	**7b**·C_7H_8	**9b**	**10b**
formula	$B_9C_{22}H_{38}NO$	$B_9C_{19}H_{32}N$	$B_{18}C_{44}H_{80}N_6Ti_2$	$B_9C_{24}H_{47}N_4Zr$	$B_9C_{26}H_{38}N$	$B_9C_{12}H_{26}N$	$B_9C_{16}H_{32}Cl_2NOZr$
fw	429.82	371.75	983.52	580.17	461.89	281.63	513.84
cryst class	orthorhombic	orthorhombic	triclinic	monoclinic	monoclinic	triclinic	triclinic
space group	*Pbca*	$P2_12_12_1$	$P\bar{1}$	$P2_1/n$	$P2_1/c$	$P\bar{1}$	$P\bar{1}$
Z	8	4	2	4	4	2	2
cell constants							
a, Å	10.712(1)	9.3362(5)	12.847(2)	11.705(1)	13.569(6)	7.9966(8)	8.235(2)
b, Å	19.056(1)	15.139(1)	12.858(2)	16.331(2)	21.536(5)	10.480(1)	11.095(3)
c, Å	25.541(2)	15.787(1)	17.658(2)	16.696(2)	9.593(3)	10.891(1)	14.200(4)
α, deg			110.720(3)			94.327(2)	102.958(6)
β, deg			91.815(3)	92.945(3)	98.66(3)	95.112(2)	103.186(5)
γ, deg			90.518(3)			110.880(2)	93.844(6)
V, Å^3	5213.7(7)	2231.4(2)	2726.0(6)	3187.2(7)	2771(2)	843.7 (2)	1221.5(6)
μ, mm^{-1}	0.059	0.057	0.331	0.366	0.057	0.055	0.678
cryst size, mm	0.40 × 0.45 × 0.55	0.40 × 0.45 × 0.45	0.32 × 0.37 × 0.43	0.30 × 0.30 × 0.30	0.35 × 0.40 × 0.40	0.28 × 0.26 × 0.20	0.25 × 0.20 × 0.18
D_{calcd}, g/cm^3	1.075	1.107	1.198	1.209	1.088	1.109	1.397
F(000)	1776	792	1040	1216	952	300	524
radiation	Mo Kα ($\lambda = 0.7107$), $T = 293(2)$ K						
θ range, deg	1.59−25.97	1.86−25.97	1.23−23.28	1.75−28.32	1.52−25.97	1.89−28.35	1.90−28.28
h,*k*,*l* collected	+13, +23, +31	+11, +18, +19	$-14 \le h \le 17$, $-16 \le k \le 17$, $-21 \le l \le 23$	$-11 \le h \le 15$, $-21 \le k \le 21$, $-21 \le l \le 22$	±16, +26, +11	$-10 \le h \le 10$, $-13 \le k \le 14$, $-14 \le l \le 14$	$-10 \le h \le 10$, $-8 \le k \le 14$, $-18 \le l \le 16$
no. of rflns measd	5105	2491	20 176	23 074	5772	11 496	8846
no. of unique rflns	5105	2491	13 343	7914	5430	4189	5953
no. of rflns used in refinement ($I > 2\sigma(I)$)	1521	1166	5195	3675	1109	2494	3142
no. of params	288	274	659	359	338	203	281
R1[a] ($I > 2\sigma(I)$)	0.1391	0.0925	0.0660	0.0678	0.1095	0.0658	0.0470
wR2[a] (all data)	0.4492	0. 3393	0.1670	0.1651	0.3077	0.2319	0.0952
GOF	1.051	1.026	0.917	0.979	0.911	1.054	0.820

[a] $R1 = \sum||F_o| - |F_c|| / \sum|F_o|$ (based on reflections with $F_o^2 > 2\sigma F^2$). [b] $wR2 = [\sum[w(F_o^2 - F_c^2)^2]/\sum[w(F_o^2)^2]]^{1/2}$; $w = 1/[\sigma^2(F_o^2) + (0.095P)^2]$; $P = [\max(F_o^2, 0) + 2F_c^2]/3$ (also with $F_o^2 > 2\sigma F^2$).

Table 3. Selected Interatomic Distances (Å) for Compounds 2a·C_4H_8O, 2b, 5a, 6a, 7b·C_7H_8, 9b, and 10b

Compound **2a**·C_4H_8O									
C(9)−C(10)	1.51(1)	N(1)−C(10)	1.491(9)	N(1)−C(11)	1.51(1)	N(1)−C(18)	1.519(9)	C(7)−C(9)	1.52(1)
C(11)−C(12)	1.51(1)	C(18)−C(19)	1.51(1)						
Compound **2b**									
C(7)−C(10)	1.53(1)	C(10)−C(11)	1.53(1)	N(1)−C(11)	1.52(1)	N(1)−C(12)	1.51(1)	N(1)−C(19)	1.51(1)
C(12)−C(13)	1.45(1)	C(19)−C(20)	1.50(1)						
Compound **5a**									
Ti(1)−N(1)	2.319(3)	Ti(1)−N(2)	1.896(3)	Ti(1)−N(3)	1.916(3)	Ti(1)−C(7)	2.423(4)	Ti(1)−C(8)	2.418(4)
Ti(1)−B(9)	2.386(4)	Ti(1)−B(10)	2.427(4)	Ti(1)−B(11)	2.402(4)	N(1)−C(10)	1.474(4)	N(1)−C(11)	1.517(4)
N(1)−C(18)	1.540(4)	N(2)−C(25)	1.472(4)	N(2)−C(26)	1.456(4)	N(3)−C(27)	1.471(5)	N(3)−C(28)	1.461(5)
Ti(1′)−N(1′)	2.310(3)	Ti(1′)−N(2′)	1.888(4)	Ti(1′)−N(3′)	1.901(3)	Ti(1′)−C(7′)	2.400(4)	Ti(1′)−C(8′)	2.426(4)
Ti(1′)−B(9′)	2.408(5)	Ti(1′)−B(10′)	2.435(5)	Ti(1′)−B(11′)	2.405(5)	N(1′)−C(10′)	1.495(5)	N(1′)−C(11′)	1.543(5)
N(1′)−C(18′)	1.515(5)	N(2′)−C(25′)	1.445(6)	N(2′)−C(26′)	1.479(6)	N(3′)−C(27′)	1.466(5)	N(3′)−C(28′)	1.457(5)
Compound **6a**									
Zr(1)−N(2)	2.029(4)	Zr(1)−N(3)	2.020(4)	Zr(1)−N(4)	2.363(4)	Zr(1)−C(7)	2.583(4)	Zr(1)−C(8)	2.557(4)
Zr(1)−B(9)	2.519(5)	Zr(1)−B(10)	2.515(5)	Zr(1)−B(11)	2.558(5)	N(1)−C(10)	1.475(6)	N(1)−C(11)	1.473(5)
N(1)−C(18)	1.460(5)	N(2)−C(25)	1.428(8)	N(2)−C(26)	1.441(9)	N(3)−C(27)	1.401(7)	N(3)−C(28)	1.438(7)
N(4)−C(29)	1.451(7)	N(4)−C(30)	1.455(6)						
Compound **7b**·C_7H_8									
N(1)−B(11)	1.57(1)	C(7)−C(10)	1.49(1)	C(10)−C(11)	1.534(9)	N(1)−C(11)	1.536(8)	N(1)−C(19)	1.520(8)
N(1)−C(12)	1.522(8)								
Compound **9b**									
C(8)−C(10)	1.527(3)	C(10)−C(11)	1.514(3)	N(1)−C(11)	1.500(3)	N(1)−C(12)	1.508(3)	C(12)−C(13)	1.504(3)
Compound **10b**									
Zr(1)−N(1)	2.349(3)	Zr(1)−Cl(1)	2.419(1)	Zr(1)−Cl(2)	2.409(1)	Zr(1)−0(1)	2.276(3)	Zr(1)−C(7)	2.749(4)
Zr(1)−C(8)	2.726(4)	Zr(1)−B(9)	2.500(4)	Zr(1)−B(10)	2.379(4)	Zr(1)−B(11)	2.488(4)	C(8)−C(10)	1.533(5)
C(10)−C(11)	1.523(5)	N(1)−C(11)	1.470(4)	N(1)−C(12)	1.512(4)				

Selected bond lengths and angles for **7a** are listed in Tables 3 and 4. The formation of a stable five-membered exocyclic ring involving the (dibenzylamino)ethyl unit is indicated in the ^{1}H NMR spectra by a downfield shift of the methylene protons of the side chain as well as the presence of diastereotopic methylene proton signals. Furthermore, identification of the B−H−B resonance implies that this compound has a zwitterionic nature.

Complex **7** can be obtained with good repeatability by exposing a preformed solution of ($Dcab^{C(2)N}$)$TiCl_2$ (**3**) to either normal (i.e., moist) or P_2O_5-dried air. The controlled nature and specificity of this nitrogen sub-

Table 4. Selected Interatomic Angles (deg) for Compounds 2a·C_4H_8O, 2b, 5a, 6a, 7b·C_7H_8, 9b, and 10b

			Compound **2a·C_4H_8O**				
C(10)−C(9)−C(7)	111.3(7)	N(1)−C(10)−C(9)	116.9(7)	C(10)−N(1)−C(11)	112.9(6)	C(10)−N(1)−C(18)	111.1(6)
C(11)−N(1)−C(18)	110.5(6)	C(12)−C(11)−N(1)	113.4(6)	C(19)−C(18)−N(1)	113.9(5)		
			Compound **2b**				
C(11)−C(10)−C(7)	114.2(7)	N(1)−C(11)−C(10)	114.1(7)	C(19)−N(1)−C(11)	112.6(6)	C(12)−N(1)−C(11)	109.7(7)
C(12)−N(1)−C(19)	112.9(7)	C(13)−C(12)−N(1)	115.6(8)	C(20)−C(19)−N(1)	114.8(7)		
			Compound **5a**				
N(2)−Ti(1)−N(1)	16.4(1)	N(3)−Ti(1)−N(1)	95.6(1)	N(2)−Ti(1)−N(3)	100.1(1)	C(10)−C(9)−C(8)	112.3(3)
N(1)−C(10)−C(9)	111.2(3)	C(10)−N(1)−Ti(1)	108.8(2)	C(10)−N(1)−C(18)	112.6(3)	C(10)−N(1)−C(11)	110.3(3)
C(11)−N(1)−C(18)	111.2(3)	C(26)−N(2)−C(25)	108.9(3)	C(25)−N(2)−Ti(1)	125.4(2)	C(28)−N(3)−C(27)	108.3(3)
C(27)−N(3)−Ti(1)	117.4(2)	N(2′)−Ti(1′)−N(1′)	103.1(1)	N(3′)−Ti(1′)−N(1′)	93.2(1)	N(2′)−Ti(1′)−N(3′)	102.5(2)
C(10′)−C(9′)−C(8′)	114.2(4)	N(1′)−C(10′)−C(9′)	111.0(3)	C(10′)−N(1′)−Ti(1′)	105.1(2)	C(10′)−N(1′)−C(18′)	110.8(3)
C(10′)−N(1′)−C(11′)	110.9(3)	C(18′)−N(1′)−C(11′)	110.4(3)	C(25′)−N(2′)−C(26′)	107.3(4)	C(25′)−N(2′)−Ti(1′)	126.2(3)
C(28′)−N(3′)−C(27′)	107.5(3)	C(27′)−N(3′)−Ti(1′)	117.3(3)				
			Compound **6a**				
N(3)−Zr(1)−N(2)	107.1(2)	N(2)−Zr(1)−N(4)	100.4(2)	N(3)−Zr(1)−N(4)	96.8(2)	C(10)−C(9)−C(7)	117.6(4)
N(1)−C(10)−C(9)	110.4(4)	C(18)−N(1)−C(11)	111.2(3)	N(1)−C(11)−C(12)	114.0(4)	N(1)−C(18)−C(19)	111.3(4)
C(25)−N(2)−C(26)	103.2(6)	C(25)−N(2)−Zr(1)	127.6(4)	C(27)−N(3)−C(28)	105.7(5)	C(27)−N(3)−Zr(1)	116.5(4)
C(29)−N(4)−C(30)	109.6(4)	C(29)−N(4)−Zr(1)	117.0(4)				
			Compound **7b**·C_7H_8				
C(7)−C(10)−C(11)	105.8(6)	C(10)−C(11)−N(1)	107.3(6)	C(12)−N(1)−C(11)	112.0(6)	C(19)−N(1)−C(11)	111.9(6)
C(11)−N(1)−B(11)	103.2(6)	C(19)−N(1)−C(12)	107.7(6)	C(12)−N(1)−B(11)	113.8(6)	C(19)−N(1)−B(11)	108.2(6)
C(20)−C(19)−N(1)	117.4(6)	N(1)−C(12)−C(13)	114.8(6)				
			Compound **9b**				
C(11)−C(10)−C(8)	111.0(2)	N(1)−C(11)−C(10)	111.6(2)	C(11)−N(1)−C(12)	112.8(2)	C(13)−C(12)−N(1)	111.9(2)
			Compound **10b**				
N(1)−Zr(1)−Cl(1)	81.52(8)	N(1)−Zr(1)−Cl(2)	80.81(8)	0(1)−Zr(1)−N(1)	145.8(1)	0(1)−Zr(1)−Cl(1)	81.29(8)
Cl(2)−Zr(1)−Cl(1)	117.02(5)	0(1)−Zr(1)−Cl(2)	81.05(9)	C(11)−C(10)−C(8)	114.5(3)	N(1)−C(11)−C(10)	111.7(3)
C(11)−N(1)−Zr(1)	113.7(2)	C(11)−N(1)−C(12)	110.2(3)	C(12)−N(1)−Zr(1)	115.0(2)		

Scheme 6. Proposed Reaction Sequence for the Formation of Fused B,N-Exocyclic Dicarbollyl Compounds 7[a]

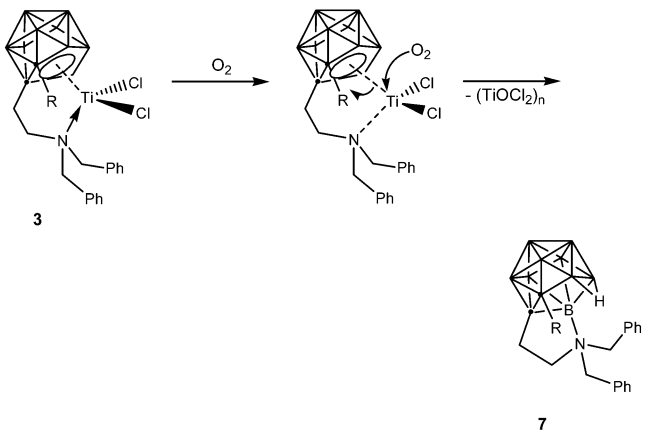

stitution are remarkable. Although the precise mechanism for the formation of **7** is not yet known, the observations noted above suggest that nitrogen insertion is either directly templated or else that, in the conversion of **3** to **7**, the processes of fused ring formation and nitrogen substitution occur concurrently (Scheme 6). It is quite possible that the amine nitrogen atom of ($Dcab^N$)$TiCl_2$ (**3**) does not remain bound to Ti but rather becomes coordinated to an electrophilic B center in the open-cage boranes. The facile demetalation observed for ($Dcab^{C(2)N}$)$TiCl_2$ (**3**) is partly due to steric crowding around the metal center caused by the two bulky dibenzyl units on the amino nitrogen atom. The formation of **7** may be mediated by titanium, and similar metal-mediated substitution reactions of the cage B−H bond have been reported.[9a,12,15]

(15) Kang, H. C.; Lee, S. S.; Knobler, C. B.; Hawthorne, M. F. *Inorg. Chem*. **1991**, *30*, 2024 and references therein.

Scheme 7. Synthesis of Sterically Less Protected (Monobenzyl)amino CGC-Type Complexes[a]

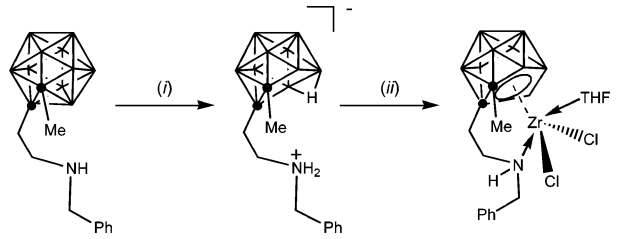

[a] Conditions: (i) (a) KOH, EtOH, 78 °C; (b) H_3PO_4, benzene, 25 °C, 10 h; (ii) (a) KH, THF, 0 °C; (b) $ZrCl_4$, toluene, −78 °C.

We hypothesized that the presence of two benzyl groups on the nitrogen atom leads to excessive steric crowding on the metal center, which in turn causes demetalation. Therefore, we devised a monobenzylated amine derivative in order to synthesize the corresponding CGC-type complexes. The synthesis of the corresponding monobenzylated amino-tethered compound **8b** has been described previously.[6] Successful deborination followed by metalation opens the possibility of accessing new types of CGC species with less steric crowding, as depicted in Scheme 7. An X-ray analysis of **9b** (Figure 7) revealed that it adopts a monomeric structure. The structural features of **9b** are similar to those of its parent dibenzyl compound **2b**, except for the detachment of one benzyl unit from the amino functionality. The reaction of **9b** with zirconium chloride complexes resulted in the formation of new types of constrained species, which could be isolated and studied spectroscopically. Of course, the reduction in steric crowding due to the presence of a single benzyl group instead of two such groups enables better interaction between the N atom and the metal. Thus, removal of one benzyl group from the (dibenzylamino)ethyl sidearm to give a

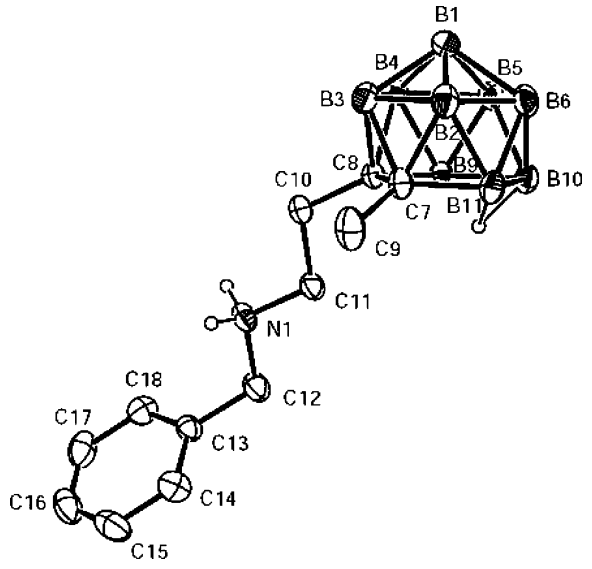

Figure 7. Molecular structure of **9b** with thermal ellipsoids drawn at the 30% level.

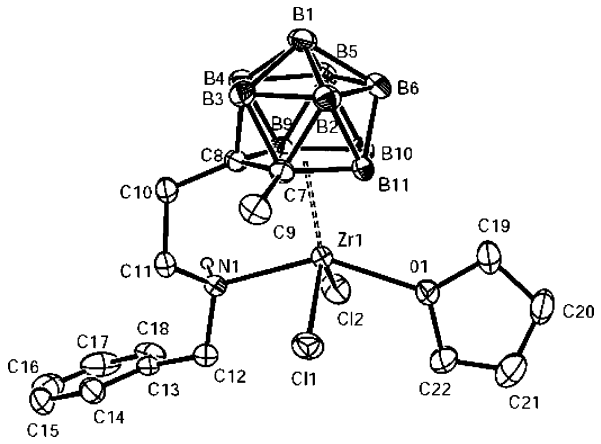

Figure 8. Molecular structure of **10b** with thermal ellipsoids drawn at the 30% level.

monobenzylated form results in the formation of a new type of constrained-geometry complex, [{(η^5-$CH_3C_2B_9H_9$)-(CH_2)(η^1-NBz)}$ZrCl_2$] (**10b**; Scheme 7).

Complex **10b** was identified by examining its ^{1}H and ^{13}C NMR spectra, which display features almost identical with those of **3** and **4**. The coordination of the nitrogen atoms of the amine to the titanium was evident from the downfield shift of the aminoethyl protons in the ^{1}H NMR spectrum. In addition, the C_1 symmetry of **10b** was evident from the appearance of an AB pattern for the bridgehead ethylene groups of the coordinated dibenzylamino unit. Furthermore, the multiplicity of the spin system of the NCH_2 moiety changes from a singlet for the free side chain to an AB spin system upon coordination to the zirconium atom, because of the restricted conformational freedom. A single-crystal X-ray structure determination of **10b** (Figure 8, with pertinent interatomic distances and angles in Tables 3 and 4) shows that it has a four-legged piano-stool structure, with the coordinated amine and the THF in a trans geometry. In **10b**, the sterically demanding phenyl group of the benzyl unit is bent away from the zirconium metal center; this minimizes steric hindrance associated with placing the N(1)−C(6) vector in the gauche orientation with respect to two Zr−Cl bonds and results in a larger Cl(1)−Zr(1)−Cl(2) angle of 117.01(5)° and a shorter Zr(1)−N(1) bond of 2.352(3) Å (versus 113.0(1)° and 2.465(3) Å in the related Cp analogue [{(η^5-C_5H_5)($SiMe_2$)(η^1:η^1-$NCH_2CH_2NMe_2$)}$ZrCl_2$] with the secondary amine).[16] The Zr−(C_2B_3 centroid) distance (2.137 Å) in **10b** is 0.03 Å longer than that in the side amino noncoordinated congener **6a** (2.109 Å), due to the higher coordination number. The coordination of the HNB_z functionality in **10b** contrasts with the noncoordination of the tertiary amine functionalities in complexes **6**, as observed above. In the former complex this is likely to be caused by an unfavorable interaction between the bulky dibenzylamino group and the metal center and in the latter possibly by a reduced ability to avoid steric hindrance with the less bulky monobenzyl unit on the amino nitrogen atom.

Conclusions

We have demonstrated that a series of CGC-type group 4 metal complexes can easily be prepared when the dibenzylamino group is tethered to the dicarbollyl ligand. The presence of bulky groups on the sidearm blocked additional coordination sites at the metal center, thereby favoring the formation of mono- rather than bis(amino)dicarbollylmetal complexes via the introduction of ancillary donor ligands, such as the dibenzylamino unit in the present case. In addition, the results show a significant substituent effect; specifically, steric hindrance caused by the bulky dibenzylamino groups leads to distortion of the titanium atom from the center of the C_2B_3 bonding face of the dicarbollyl unit, whereas the less bulky monobenzylated group does not cause this distortion. As a result, the mono(aminodicarbollyl)-titanium species **3** are unstable and react further with molecular oxygen to produce the thermodynamically more stable exocyclic dicarbollides **7**. Another attractive feature of the (dibenzylamino)ethyl dicarbollyl ligand is the tailorability of the dibenzyl unit on the donor sidearm via debenzylation. Removal of one benzyl group from the dibenzyl unit reduced steric congestion around the metal center, thereby producing stable CGC-type group metal complexes such as **10b**.

Experimental Section

General Procedures. All manipulations were performed under a dry, oxygen-free nitrogen or argon atmosphere using standard Schlenk techniques or in a Vacuum Atmospheres HE-493 drybox. THF, diethyl ether, toluene, hexane, and pentane were distilled under nitrogen from sodium/benzophenone. Dichloromethane was dried with CaH_2. Benzene-d_6 was distilled under nitrogen from sodium and stored in a Schlenk storage flask until needed. $CDCl_3$ was predried under CaH_2 and vacuum-transferred. KH, *n*-BuLi (1.6 M in hexanes), MCl_4 (M = Ti, Zr), and Me_3SiCl were used as received from Aldrich and Strem. *o*-Carborane was purchased from Katechem and used after sublimation. M(NMe_2)$_4$ (M = Ti, Zr)[17] and compounds **1** and **8b** were prepared by literature methods.[6] All other reagents were obtained from commercial suppliers (Aldrich and TCI) and used as received. ^{1}H, ^{11}B, and^{13}C NMR spectra were recorded on a Varian Mercury 300 spectrometer operating at 300.1, 96.3, and 75.4 MHz, respec-

(16) Alt, H. G.; Föttinger, K.; Milius, W. *J. Organomet. Chem*. **1998**, *564*, 115.

(17) Diamond, G. M.; Jordan, R. F.; Peterson, J. L. *J. Am. Chem. Soc*. **1996**, *118*, 8024.

tively. All ^{11}B chemical shifts were referenced to $BF_3{\cdot}O(C_2H_5)_2$ (0.0 ppm) with a negative sign indicating an upfield shift. All proton and carbon chemical shifts were measured relative to internal residual peaks from the lock solvent (99.5% $(CD_3)_2SO$, 99.9% $CDCl_3$, and 99.5% C_6D_6) and then referenced to Me_4Si (0.00 ppm). IR spectra were recorded on a Biorad FTS-165 spectrophotometer. Elemental analyses were performed with a Carlo Erba Instruments CHNS-O EA1108 analyzer. All melting points were uncorrected. High-resolution mass spectra were measured at the Korea Basic Science Institute.

Preparation of [*nido*-7-NHBz$_2$$^+$(CH$_2$)$_2$-8-H-7,8-C$_2B_9H_{10}$$^-$] (2a). A representative procedure is as follows. Compound **1a** (1.47 g, 4.0 mmol) was dissolved in degassed EtOH (100 mL), and the reaction mixture was heated at reflux for 12 h. The EtOH was removed under reduced pressure, leaving a white solid material. This solid was made into a slurry by mixing with benzene (30 mL) under N_2, and H_3PO_4 was added to this slurry. The resulting two-phase mixture was stirred vigorously for 15 h, after which the benzene supernant was decanted via syringe. Removal of the solvent in vacuo and washing with light petroleum ether afforded the zwitterion of **2a** as a yellow-tinted powder. The crude product was further purified by recrystallization from THF/diethyl ether to yield **2a** (1.21 g, 3.4 mmol) as a colorless crystalline solid in 85% yield. Mp: 200 °C dec. Anal. Calcd for $B_9C_{18}H_{30}N$: C, 60.43; H, 8.45; N, 3.92. Found: C, 60.62; H, 8.47; N, 3.94. IR (KBr pellet, cm^{-1}): 3094 w (ν_{CH}), 2538 s (ν_{BH}).

[*nido*-7-NHBz$_2$$^+$(CH$_2$)$_2$-8-Me-7,8-C$_2B_9H_{10}$$^-$] (2b). A procedure similar to that used to prepare **2a** was employed, but with the following quantities: compound **1b** (1.53 g, 4.0 mmol). Yield: 88% (1.31 g, 3.5 mmol). Mp: 211 °C dec. Anal. Calcd for $B_9C_{19}H_{32}N$: C, 61.38; H, 8.68; N, 3.77. Found: C, 61.61; H, 8.65; N, 3.76. IR (KBr pellet, cm^{-1}): 3071 s, 2959 w, 2930 w, 2868 w, 2852 w (ν_{CH}), 2527 s (ν_{BH}).

Preparation of [{(η^5-RC$_2$B$_9$H$_9$)(CH$_2$)$_2$(η^1-NBz$_2$)}MCl$_2$] (M = Ti (3), Zr (4); R = H (a), Me (b)). To a stirred solution of **2a** (0.89 g, 2.5 mmol) in THF (20 mL) was added 0.22 g of KH (2.2 equiv). The mixture was stirred for 6 h at room temperature. The resulting clear yellow supernatant was decanted via syringe. Removal of the solvent in vacuo and washing with light petroleum ether afforded the dianion of **2a** as a yellow-tinted powder. To a stirred solution of $TiCl_4$ (0.47 g, 2.5 mmol) in 20 mL of toluene at −78 °C was added a stirred suspension of the dianion of **2a** in toluene (20 mL) by cannula for 30 min. After addition was complete, the cold bath was removed and the solution was stirred at room temperature for 2 h. The formation of **2a** was demonstrated by ^1H NMR spectroscopy. Removal of the volatiles provided the final crude product. Extraction of the residue with toluene (20 mL), followed by concentration to approximately half its volume and cooling to −15 °C, resulted in crystallization of a pure reddish solid, **3a** (0.32 g, 0.67 mmol, 27% yield). Mp: 134 °C dec. HRMS: calcd for $^{12}C_{18}{}^{11}B_9{}^1H_{28}{}^{14}N^{48}Ti^{35}Cl_2$ *m/e* 475.1916, found *m/e* 475.1893. IR (KBr, pellet, cm^{-1}): 3097 w, 3054 w, 2973 w, 2878 w (ν_{CH}), 2523 s, 2520 w (ν_{BH}).

3b. A procedure similar to that described above for compound **3a** was employed, but with the following quantities: compound **2b** (0.93 g, 2.5 mmol). Yield: 29% (0.35 g, 0.72 mmol). Mp: 149 °C dec. HRMS: calcd for $^{12}C_{19}{}^{11}B_9{}^1H_{30}{}^{14}N^{48}Ti^{35}Cl_2$ *m/e* 489.2072, found *m/e* 489.2051. IR (KBr, pellet, cm^{-1}): 3041 w, 3018 w, 2931 w (ν_{CH}), 2529 w, 2517 s (ν_{BH}).

4a. A procedure analogous to the preparation of **3a** was used, but starting from 2.5 mmol (0.58 g) of $ZrCl_4$. Yield: 25% (0.32 g, 0.62 mmol). Mp: 152 °C dec. HRMS: calcd for $^{12}C_{18}{}^{11}B_9{}^1H_{28}{}^{14}N^{91}Zr^{35}Cl_2$ *m/e* 517.1483, found *m/e* 517.1502. IR (KBr pellet, cm^{-1}): 3067 w, 3013 w, 2977 w, 2900 w (ν_{CH}), 2527 s, 2512 w (ν_{BH}).

4b. A procedure analogous to the preparation of **4a** was used, but starting from 2.5 mmol of **2b**. Yield: 23% (0.31 g, 0.58 mmol). Mp: 150 °C dec. HRMS: calcd for $^{12}C_{19}{}^{11}B_9{}^1H_{30}{}^{14}N^{91}Zr^{35}Cl_2$ *m/e* 531.1640, found *m/e* 531.1620. IR (KBr pellet, cm^{-1}): 3074 w, 2940 w (ν_{CH}), 2522 s (ν_{BH}).

Preparation of [{(η^5-C$_2$B$_9$H$_{10}$)(CH$_2$)$_2$(η^1-NBz$_2$)}Ti(NMe$_2$)$_2$] (5a). Over a period of 30 min, a 20 mL toluene solution of $Ti(NMe_2)_4$ (0.22 g, 1.0 mmol) was added to a stirred solution of **2a** (0.36 g, 1.0 mmol) in toluene (20 mL) at 0 °C. After addition was complete, the cold bath was removed and the solution was stirred at room temperature for 1 h. Solvent was removed in vacuo and the residue purified by recrystallization with toluene at −15 °C. Red crystalline solid. Yield: 73% (0.36 g, 0.73 mmol). Mp: 147 °C dec. HRMS calcd for $^{12}C_{22}{}^{11}B_9{}^1H_{40}{}^{14}N_3{}^{48}Ti$ *m/e* 493.3539, found *m/e* 493.3521. IR spectrum (KBr, pellet, cm^{-1}): 3084 w, 3067 w, 3030 w, 2924 w, 2795 w (ν_{CH}), 2527 s (ν_{BH}).

[{(η^5-MeC$_2$B$_9$H$_9$)(CH$_2$)$_2$(η^1-NBz$_2$)}Ti(NMe$_2$)$_2$] (5b). A procedure analogous to the preparation of **5a** was used, but starting from compound **2b** (0.37 g, 1.0 mmol). Red crystalline solid. Yield: 81% (0.41 g, 0.81 mmol). Mp: 155 °C dec. HRMS: calcd for $^{12}C_{23}{}^{11}B_9{}^1H_{42}{}^{14}N_3{}^{48}Ti$ *m/e* 507.3696, found *m/e* 507.3681. IR (KBr, pellet, cm^{-1}): 3064 w, 3037 w, 2955 w, 2930 w, 2868 w, 2772 w (ν_{CH}), 2515 s (ν_{BH}).

6a. A procedure analogous to the preparation of **5a** was used, but starting from 1.0 mmol (0.27 g) of $Zr(NMe_2)_4$. Yellow crystalline solid. Yield: 65% (0.38 g, 0.65 mmol). Mp: 149 °C dec. HRMS: calcd for $^{12}C_{24}{}^{11}B_9{}^1H_{47}{}^{14}N_4{}^{91}Zr$ *m/e* 580.3685, found *m/e* 580.3667. IR (KBr pellet, cm^{-1}): 3413 m (ν_{NH}), 3086 w, 3058 w, 3028 w, 2926 w (ν_{CH}), 2523 s (ν_{BH}).

6b. A procedure analogous to the preparation of **6a** was used, but starting from 1.0 mmol of **3b.** Yield: 72% (0.43 g, 0.72 mmol). Mp: 145 °C dec. HRMS: calcd for $^{12}C_{25}{}^{11}B_9{}^1H_{49}{}^{14}N_4{}^{91}Zr$ *m/e* 594.3842, found *m/e* 594.3818. IR (KBr pellet, cm^{-1}): 3423 w (ν_{NH}), 3167 w, 3061 w, 3028 w, 2957 w, 2930 w, 2968 w, 2799 w (ν_{CH}), 2517 s (ν_{BH}).

Preparation of Compound 3 from Compound 5. Complex **5a** (0.49 g, 1.0 mmol) was dissolved in methylene chloride (20 mL), and then an excess amount of Me_3SiCl (3.3 equiv) was added. The resulting solution was stirred for 30 min, after which all volatiles were removed under vacuum and the residue was washed with pentane three times. Removal of the volatiles provided the final crude product, which was further purified from toluene at −15 °C to provide pure complex **3a** as a red solid. Yield: 70% (0.33 g, 0.70 mmol). For **3b**, a similar procedure was employed as described for **3a**, but with the following quantities: compound **5b** (0.51 g, 1.0 mmol). Yield: 76% (0.37 g, 0.76 mmol).

Preparation of *exo-B,N-nido*-7,11-NBz^{2+}(CH$_2$)$_2$-8-H-7,8-C$_2$B$_9$H$_9$$^-$ (7a). A solution of **3a** (0.47 g, 1 mmol) in toluene was bubbled with 1 atm of pure O_2 at 0 °C for 1 h. The resulting yellow mixture was warmed to 25 °C and stirred for 2 h. ^1H NMR spectroscopy demonstrated that **7a** was formed after 5 min at room temperature. Drying of the resulting yellow solution under vacuum afforded a yellow powder. This solid was extracted with toluene, and the filtrate was concentrated to ca. 5 mL and placed at −15 °C, giving a white precipitate of **7a** which was filtered and dried in vacuo. Suitable crystals for X-ray diffraction analysis were obtained from a saturated toluene solution at −15 °C. Yield: 65% (0.23 g, 0.65 mmol). Mp: 162 °C. Anal. Calcd for $B_9C_{18}H_{28}N$: C, 60.78; H, 7.93; N, 3.94. Found: C, 61.02; H, 7.91; N, 3.93. IR spectrum (KBr pellet, cm^{-1}): 3062 w, 3043 w, 2953 w (ν_{CH}), 2531 w, 2520 s (ν_{BH}).

exo-*B,N-nido*-7,11-NBz$_2$$^+$(CH$_2$)$_2$-8-Me-7,8-C$_2B_9H_9$$^-$ (7b). A procedure similar to that described above for **7a** was employed, but with the following quantities: compound **3b** (0.49 g, 1.0 mmol). Yield: 81% (0.30 g, 0.81 mmol). Mp: 169 °C. Anal. Calcd for $B_9C_{19}H_{30}N$: C, 61.72; H, 8.18; N, 3.79. Found: C, 61.87; H, 8.21; N, 3.80. IR (KBr pellet, cm^{-1}): 3073 w, 3019 w, 2971 m (ν_{CH}), 2523 s, 2517 s, 2511 w (ν_{BH}).

Preparation of [*nido*-7-NH$_2$Bz$^+$(CH$_2$)-8-H-7,8-C$_2$B$_9$H$_{10}$$^-$] (9b). A procedure similar to that described above for the preparation of **2a** was employed, but with the following

quantities: compound **8b** (1.17 g, 4.0 mmol). Yield: 80% (0.90 g, 3.2 mmol). Mp: 300 °C dec. Anal. Calcd for $B_9C_{12}H_{26}N$: C, 51.17; H, 9.30; N, 4.97. Found: C, 51.29; H, 9.29; N, 4.99. IR (KBr pellet, cm^{-1}): 2963 w, 2923 w, 2873 w (ν_{CH}), 2523 s (ν_{BH}).

Preparation of [{(η^5-$CH_3C_2B_9H_9$)(CH_2)(η^1-NBz)}$ZrCl_2$] (10b). A procedure analogous to the preparation of **3a** was used, but with the following quantities: compound **9b** (0.70 g, 2.5 mmol), 0.30 g of KH (3.0 equiv), and 2.5 mmol (0.58 g) of $ZrCl_4$. Yellow crystalline solid. Yield: 40% (0.35 g, 0.8 mmol). Mp: 155 °C dec. HRMS: calcd for $^{12}C_{16}{}^{11}B_9{}^{1}H_{32}{}^{14}N^{16}O^{91}Zr^{35}Cl_2$ *m/e* 513.1745, found *m/e* 513.1766. Anal. Calcd for $B_9C_{12}H_{24}NCl_2Zr$: C, 37.40; H, 6.28; N, 2.73. Found: C, 37.50; H, 6.29; N, 2.72. IR (KBr pellet, cm^{-1}): 3033 w, 2963 w, 2909 w (ν_{CH}), 2532 s (ν_{BH}).

Crystal Structure Determination. Crystals of **2a**·C_4H_8O, **2b**, **5a**, **6a**, **7b**·C_7H_8, **9b**, and **10b** were obtained from toluene, sealed in glass capillaries under argon, and mounted on the diffractometer. Preiminary examination and data collection were performed using a Bruker SMART CCD detector system single-crystal X-ray diffractometer equipped with a sealed-tube X-ray source (40 kV × 50 mA) using graphite-monochromated Mo Kα radiation (λ = 0.710 73 Å). Preliminary unit cell constants were determined with a set of 45 narrow-frame (0.3° in ω) scans. The double-pass method of scanning was used to exclude any noise. The collected frames were integrated using an orientation matrix determined from the narrow-frame scans. The SMART software package was used for data collection, and SAINT was used for frame integration.[18a] Final cell constants were determined by a global refinement of *xyz* centroids of reflections harvested from the entire data set. Structure solution and refinement were carried out using the SHELXTL-PLUS software package.[18b] Detailed information is listed in Table 2.

Computational Details. Stationary points on the potential energy surface were calculated using the Amsterdam Density Functional (ADF) program, developed by Baerends et al.[19,20] and vectorized by Ravenek.[21] The numerical integration scheme applied for the calculations was developed by te Velde et al.[22,23] The geometry optimization procedure was based on the method of Versluis and Ziegler.[24] The electronic configurations of the molecular systems were described by double-ζ STO basis sets with polarization functions for the H, B, and C atoms, while triple-ζ Slater type basis sets were employed for the Si, P, and Pt atoms.[25,26] The 1s electrons of B and C, the 1s−2p electrons of Si and P, and the 1s−4d electrons of Pt were treated as frozen cores. A set of auxiliary[27] s, p, d, f, and g STO functions, centered on all nuclei, was used in order to fit the molecular density and the Coulomb and exchange potentials in each SCF cycle. Energy differences were calculated by augmenting the local exchange-correlation potential by Vosko et al.[28] with Becke's[29] nonlocal exchange corrections and Perdew's[30] nonlocal correlation corrections (BP86). Geometries were optimized including nonlocal corrections at this level of theory. First-order Pauli scalar relativistic corrections[31,32] were added variationally to the total energy for all systems. In view of the fact that all systems investigated in this work show a large HOMO−LUMO gap, a spin-restricted formalism was used for all calculations. No symmetry constraints were used.

Acknowledgment. This work was supported by Grant No. R03-2001-00030 from the Basic Research Program of the Korean Science and Engineering Foundation.

Supporting Information Available: Tables giving crystallographic data (excluding structure factors) for the structures of **2a**·C_4H_8O, **2b**, **5a**, **6a**, **7b**·C_7H_8, **9b**, and **10b** reported in this paper and listings giving optimized geometries of the crucial structures (**5a**) reported (Cartesian coordinates, in Å). This material is available free of charge via the Internet at http://pubs.acs.org.

OM048979A

(18) (a) SMART and SAINT; Bruker Analytical X-ray Division, Madison, WI, 2002. (b) Sheldrick, G. M. SHELXTL-PLUS Software Package; Bruker Analytical X-ray Division, Madison, WI, 2002.
(19) Baerends, E. J.; Ellis, D. E.; Ros, P. *Chem. Phys.* **1973**, *2*, 41.
(20) Baerends, E. J.; Ros, P. *Chem. Phys.* **1973**, *2*, 52.
(21) Ravenek, W. In *Algorithms and Applications on Vector and Parallel Computers*; te Riele, H. J. J., Dekker, T. J., van de Horst, H. A., Eds.; Elsevier: Amsterdam, The Netherlands, 1987.
(22) te Velde, G.; Baerends, E. J. *J. Comput. Chem.* **1992**, *99*, 84.
(23) Boerrigter, P. M.; te Velde, G.; Baerends, E. J. *Int. J. Quantum Chem.* **1988**, *33*, 87.
(24) Versluis, L.; Ziegler, T. *J. Chem. Phys.* **1988**, *88*, 322.
(25) Snijders, J. G.; Baerends, E. J.; Vernoijs, P. *At. Nucl. Data Tables* **1982**, *26*, 483.
(26) Vernoijis, P.; Snijders, J. G.; Baerends, E. J. *Slater Type Basis Functions for the Whole Periodic System*; Internal Report (in Dutch); Department of Theoretical Chemistry, Free University: Amsterdam, The Netherlands, 1981.
(27) Krijn, J.; Baerends, E. J. *Fit Functions in the HFS Method*; Internal Report (in Dutch); Department of Theoretical Chemistry, Free University: Amsterdam, The Netherlands, 1984.
(28) Vosko, S. H.; Wilk, L.; Nusair, M. *Can. J. Phys.* **1980**, *58*, 1200.
(29) Becke, A. *Phys. Rev. A* **1988**, *38*, 3098.
(30) (a) Perdew, J. P. *Phys. Rev. B* **1986**, *34*, 7406. (b) Perdew, J. P. *Phys. Rev. B* **1986**, *33*, 8822.
(31) Snijders, J. G.; Baerends, E. J. *Mol. Phys.* **1978**, *36*, 1789.
(32) Snijders, J. G.; Baerends, E. J.; Ros, P. *Mol. Phys.* **1979**, *38*, 1909.